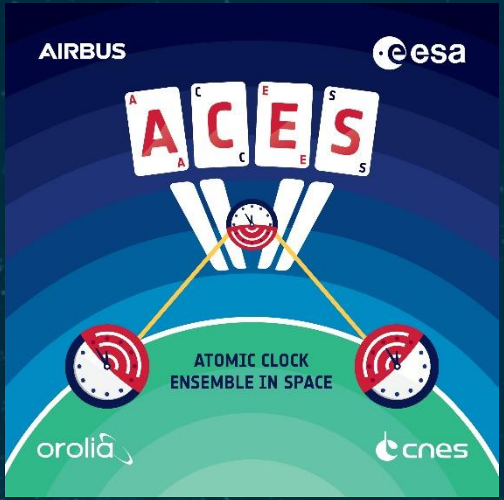

Atomic Clock Ensemble in Space

Luigi Cacciapuoti

9th Symposium on Frequency Standards and Metrology
Kingscliff – Australia

16-20 October 2023

ESA UNCLASSIFIED – For ESA Official Use Only

ACES mission concept

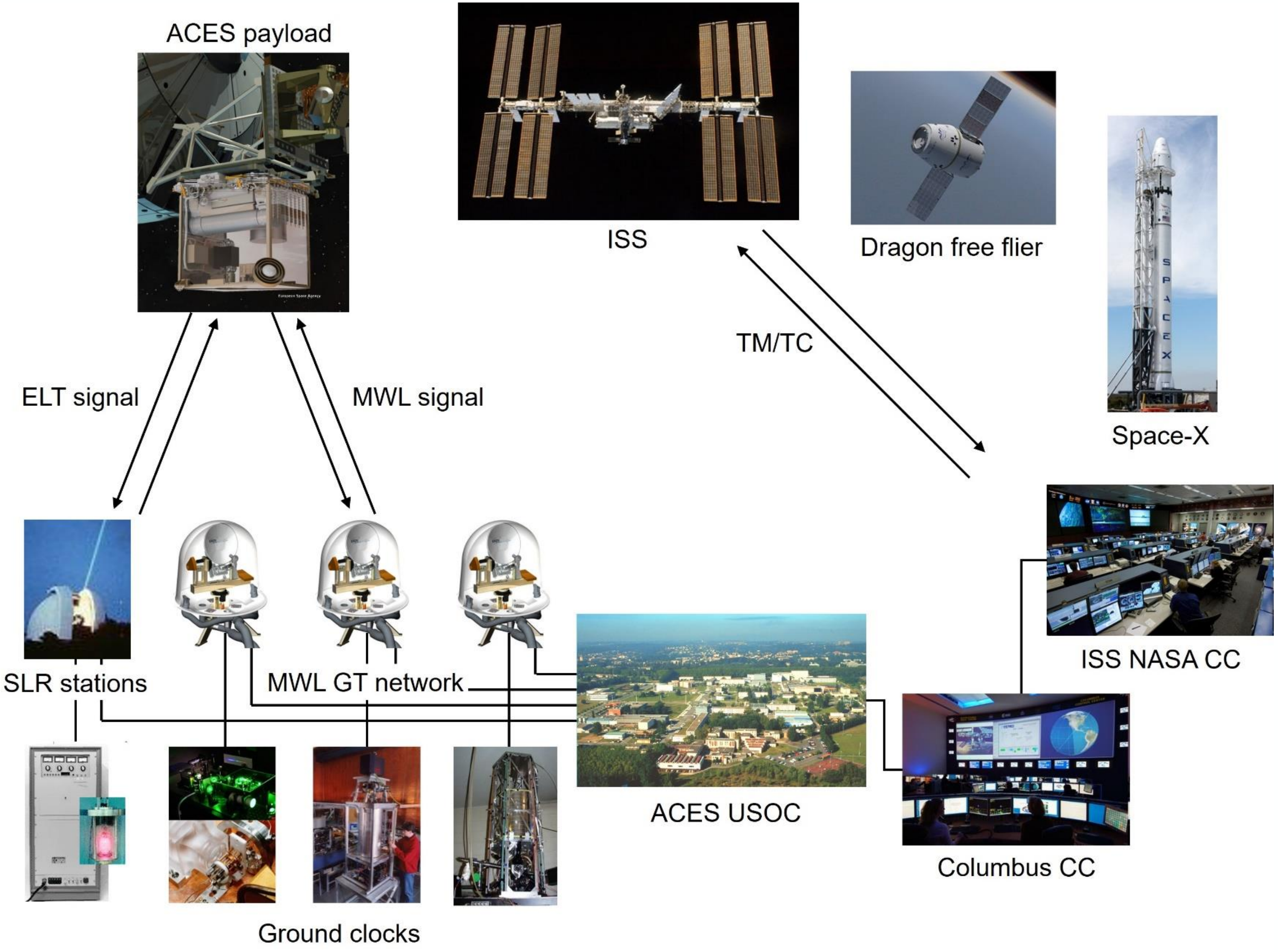

The Columbus module

The ACES payload

- **PHARAO** (CNES): Atomic clock based on laser cooled Cs atoms
- **SHM**: Active hydrogen maser
- **FCDP**: Clocks comparison and distribution
- **MWL** : T&F transfer link
- **GNSS** receiver
- **ELT**: Optical link
- **Support subsystems**
  - **XPLC**: External PL computer
  - **PDU**: Power distribution unit,
  - Mechanical, thermal subsystems
  - **CEPA**: Columbus External PL Adapter

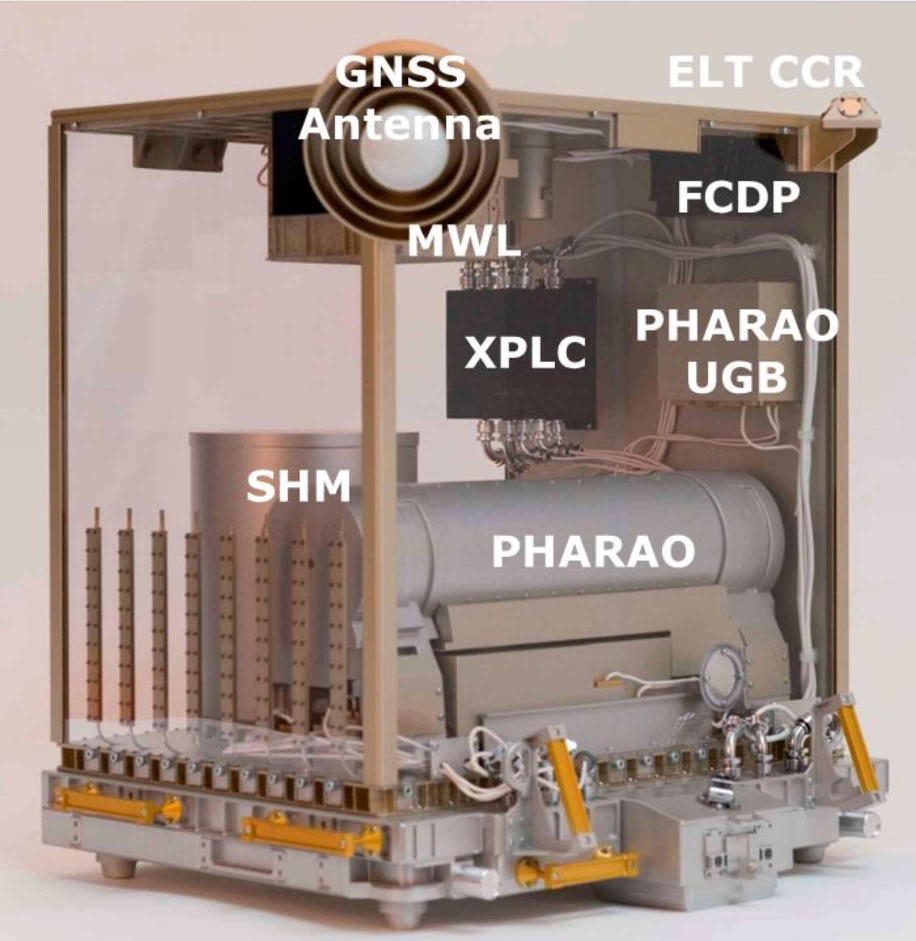

Volume: 1172x867x1246 mm^3
Mass: 240 kg (w/o CEPA)
Power: 600 W

The ACES clock signal

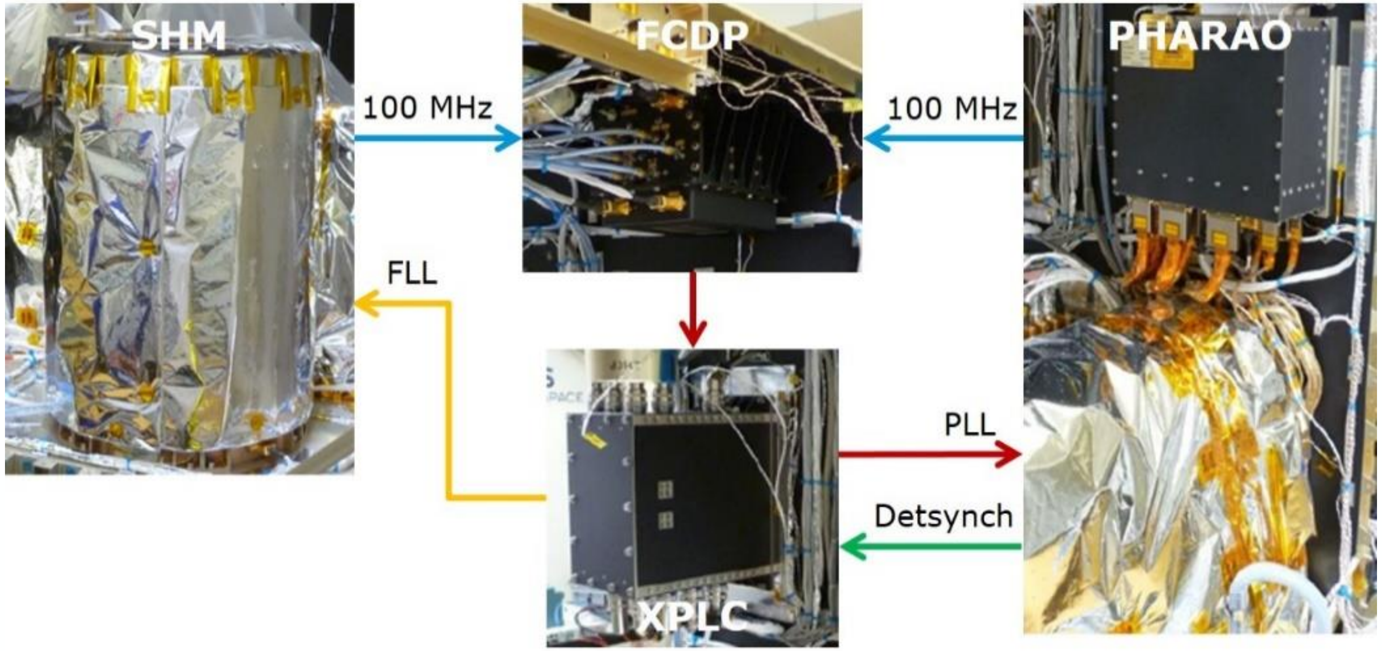

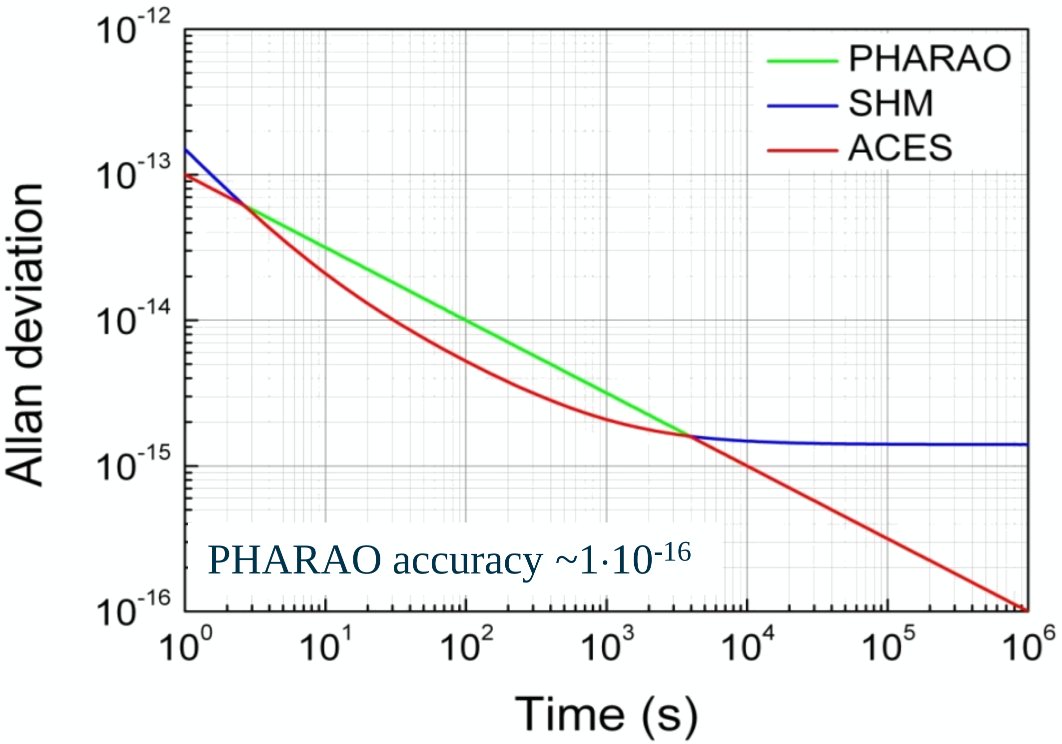

- The ACES clock signal (red curve) combines the good short-to-medium term frequency stability of the active H-maser SHM with the long-term stability and accuracy of the Cs clock PHARAO.
- Two servo-loops control the clocks with two different time constants: the short-term servo-loop (PLL) steers PHARAO local oscillator on SHM (1-2 s time constant); the long-term servo-loop (FLL) corrects SHM against long term drifts (100-500 s time constant).

PHARAO and ACES stability

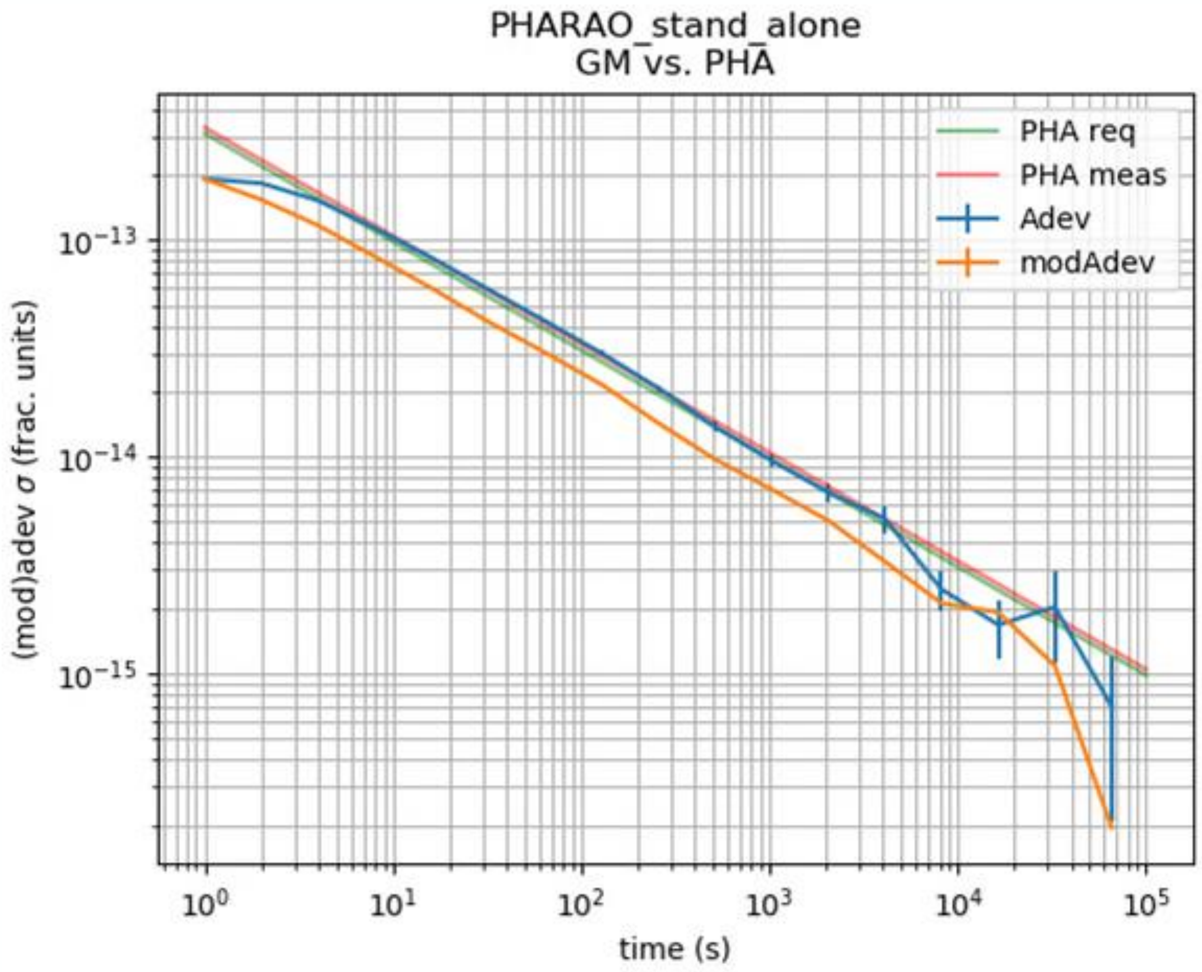

PHARAO stability in autonomous mode

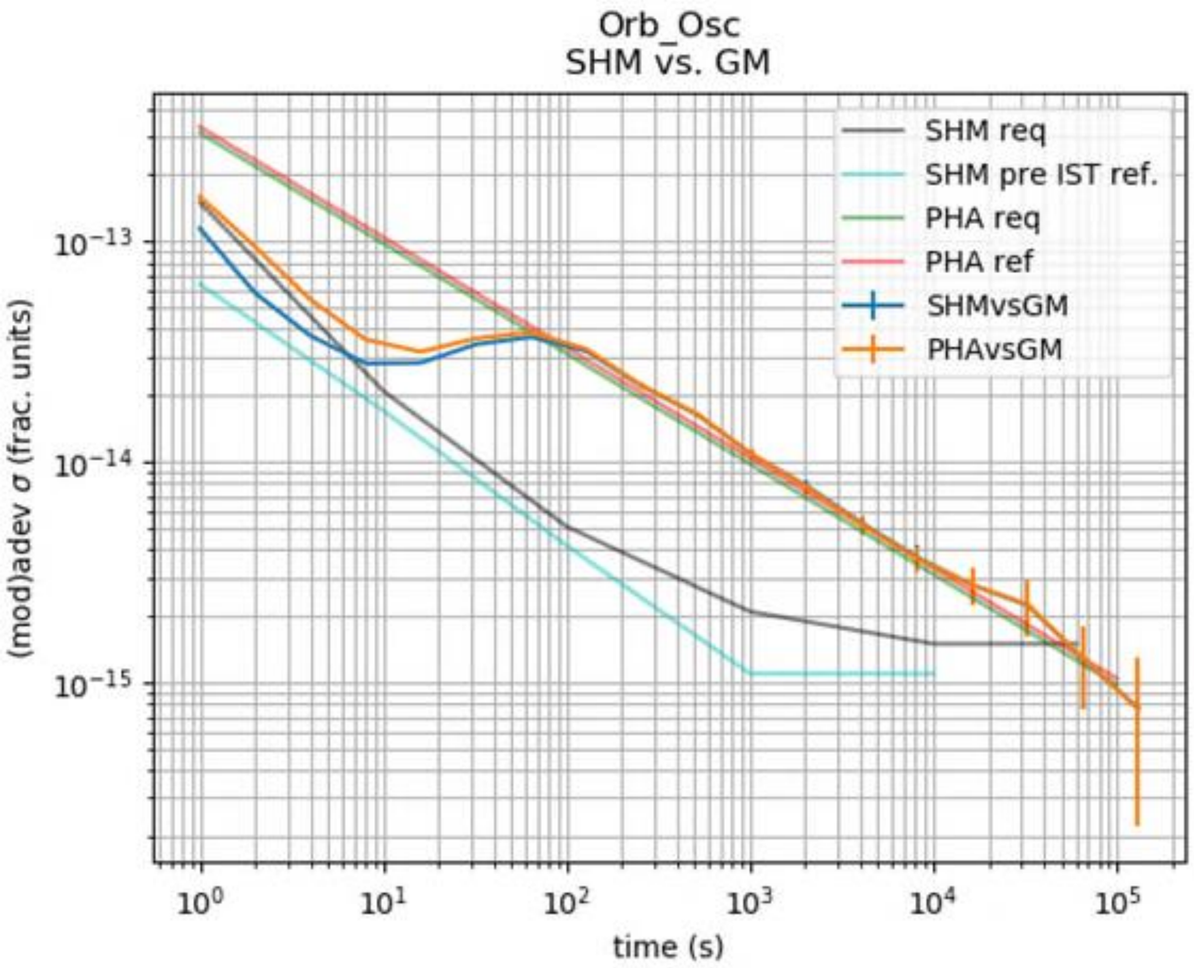

ACES stability with STSL and LTSL closed and in the presence of magnetic and thermal perturbations

ACES time & frequency links

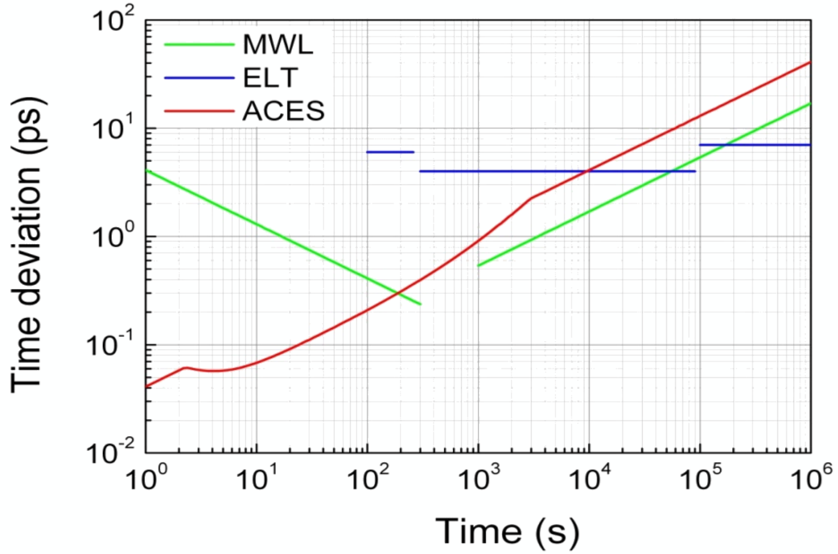

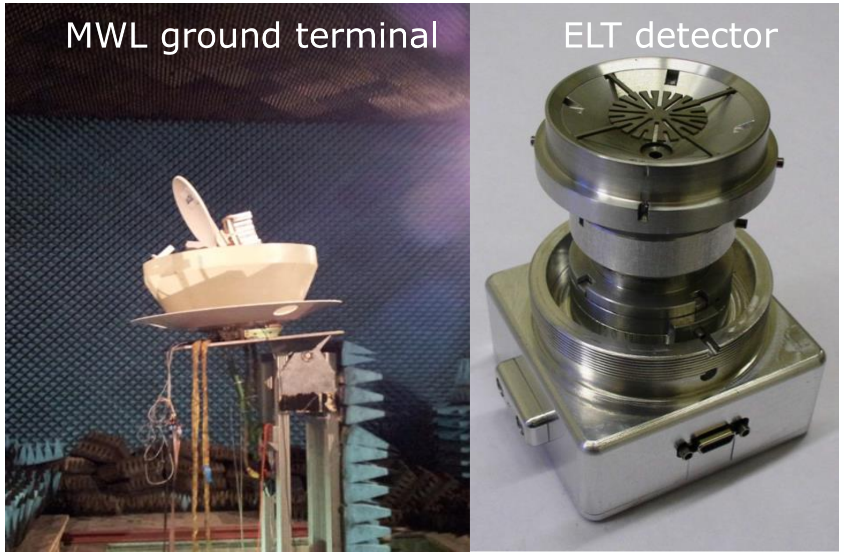

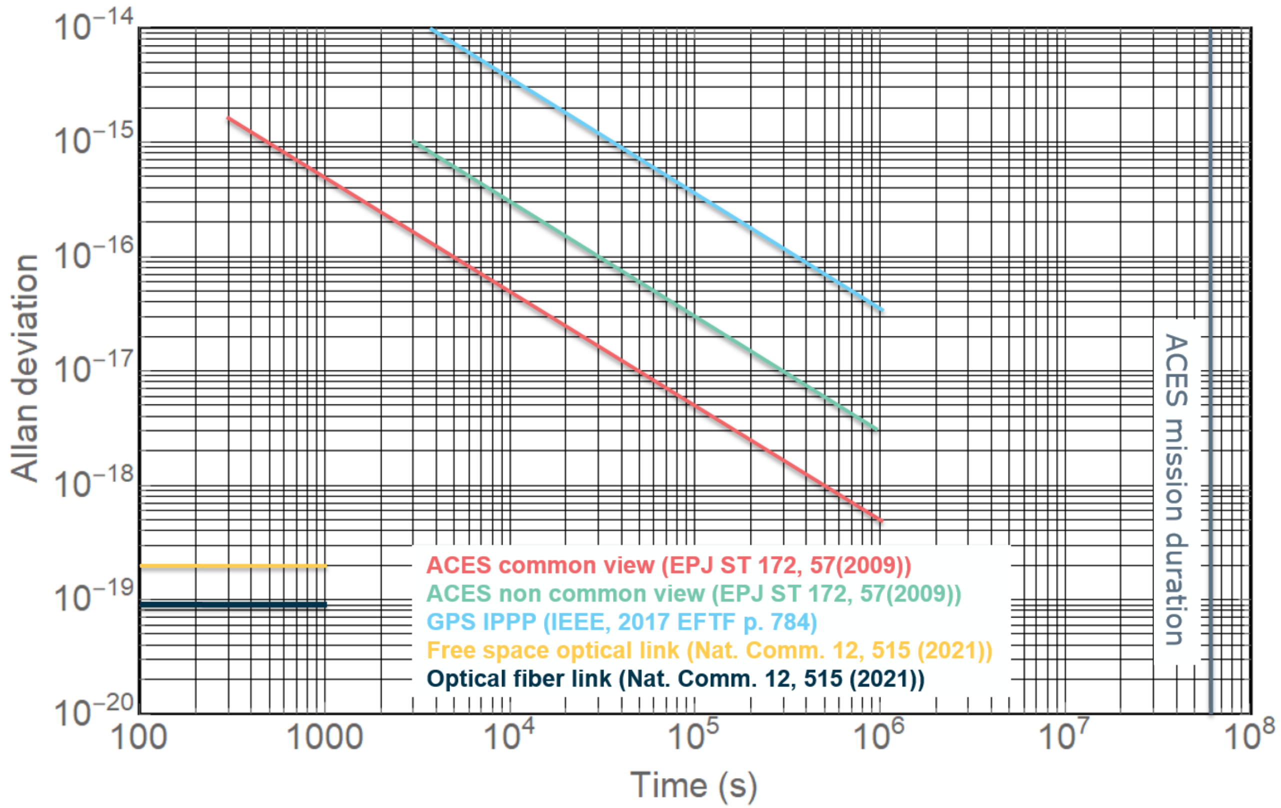

Ground clock comparisons with MWL

- **Common view:** $1.4 \cdot 10^{-15}$ after 300 s (ISS pass duration) and $1 \cdot 10^{-17}$ in less than 1 day.
- **Non common view:** $1 \cdot 10^{-15}$ after 2700 s, $1 \cdot 10^{-17}$ in 3-4 days (calculated assuming a deadtime Δt of 2700 s).

MWL

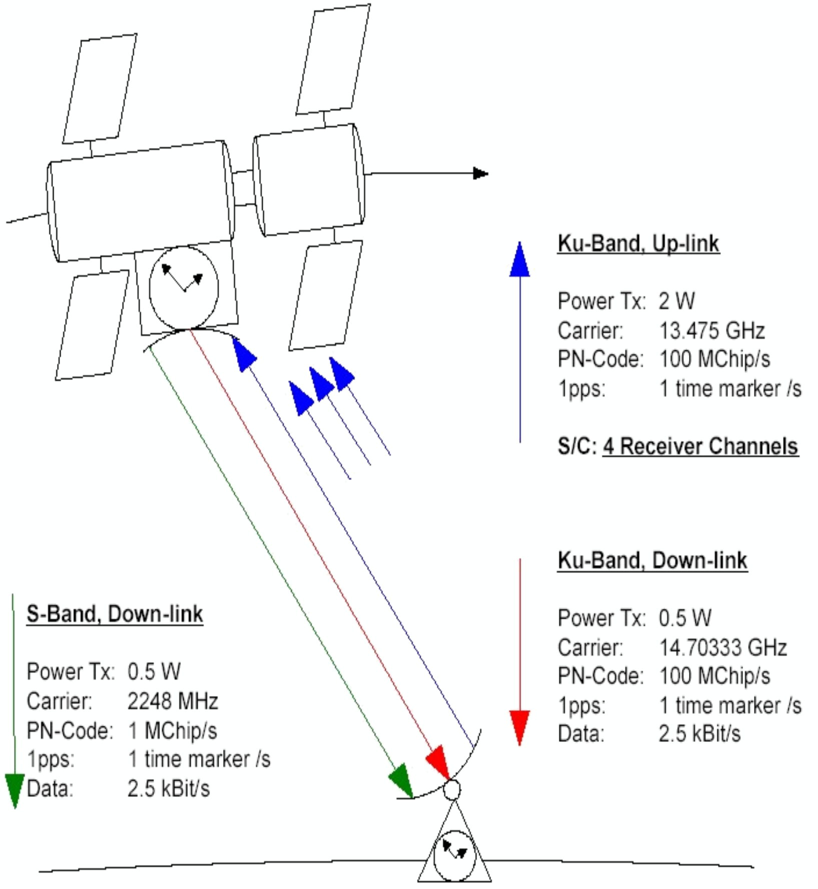

- Two-way link:
  - Removal of the troposphere time delay (8.3-103 ns)
  - Removal of 1st order Doppler effect
  - Removal of instrumental delays and common mode effects
- Additional down-link in the S-band:
  - Determination of the ionosphere TEC
  - Correction of the ionosphere time delay (0.3-40 ns in S-band, 6-810 ps in Ku-band)
- Phase PN code modulation: Removal of 2π phase ambiguity
- High chip rate (100 MChip/s) on the code:
  - Higher resolution
  - Multipath suppression
- Carrier and code phase measurements (80 ms sampling time)
- Data link: 2 kBits/s on the S-band down-link to obtain clock comparison results in real time
- Up to 4 simultaneous space-to-ground clock comparisons

MWL measurements and scientific products

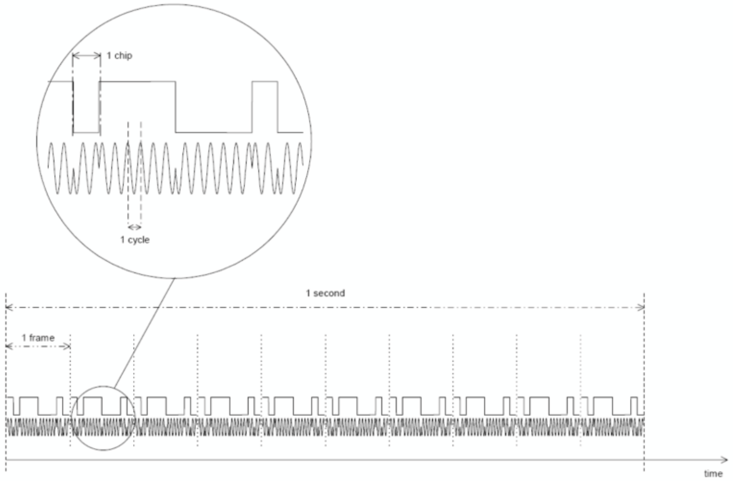

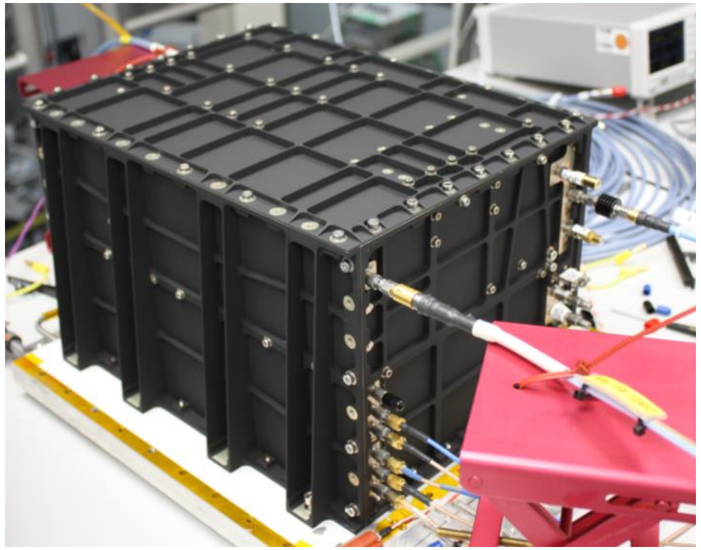

Code and carrier phase measurements on Ku-band up/down-link

$$\Delta\tau^s\left(\tau^s(t_2^o)\right) = Des(t_2^o) - \left[[\Delta^g_{T1}]^t + T_{12} + [\Delta^s_{R1}]^t\right]^g \quad \Delta\tau^g\left(\tau^g(t_4^o)\right) = -Des(t_4^o) - \left[[\Delta^s_{T2}]^t + T_{34} + [\Delta^g_{R2}]^t\right]^s$$

and S-band down-link

$$\Delta\tau^g\left(\tau^g(t_6^o)\right) = -Des(t_6^o) - \left[[\Delta^s_{T3}]^t + T_{56} + [\Delta^g_{R3}]^t\right]^s$$

where

$$\begin{cases} T_{12} = \dfrac{R_{12}}{c} + \dfrac{2GM_E}{c^3}\ln\left(\dfrac{x_g(t_1)+x_s(t_2)+R_{12}}{x_g(t_1)+x_s(t_2)-R_{12}}\right) + \Delta_{12}^{tropo} + \Delta_{12}^{iono} + O(\dfrac{1}{c^4}) \\ T_{34} = \dfrac{R_{34}}{c} + \dfrac{2GM_E}{c^3}\ln\left(\dfrac{x_g(t_4)+x_s(t_3)+R_{34}}{x_g(t_4)+x_s(t_3)-R_{34}}\right) + \Delta_{34}^{tropo} + \Delta_{34}^{iono} + O(\dfrac{1}{c^4}) \\ T_{56} = \dfrac{R_{56}}{c} + \dfrac{2GM_E}{c^3}\ln\left(\dfrac{x_g(t_6)+x_s(t_5)+R_{56}}{x_g(t_6)+x_s(t_5)-R_{56}}\right) + \Delta_{56}^{tropo} + \Delta_{56}^{iono} + O(\dfrac{1}{c^4}) \end{cases}$$

Scientific Products		**…from**
Space-to-ground Desynchronization	$\tau^g(t_a) - \tau^s(t_a)$	$\Delta\tau^s\left(\tau^s(t_2^o)\right) - \Delta\tau^g\left(\tau^g(t_4^o)\right)$
Ionosphere Total Electron Content	$(\frac{1}{f_3^2} - \frac{1}{f_2^2})\frac{40.308}{c}C_e$	$\Delta\tau^g\left(\tau^g(t_4^o)\right) - \Delta\tau^g\left(\tau^g(t_6^o)\right)$
Range + Tropospheric Delay	$D(t_4)$ & Δ_{34}^{tropo}	$\Delta\tau^s\left(\tau^s(t_2^o)\right) + \Delta\tau^g\left(\tau^g(t_4^o)\right)$

MWL PFM performance - Static

MWL Time deviation [s]: 2-way combination of common clock measurements under static conditions (no signal dynamics)

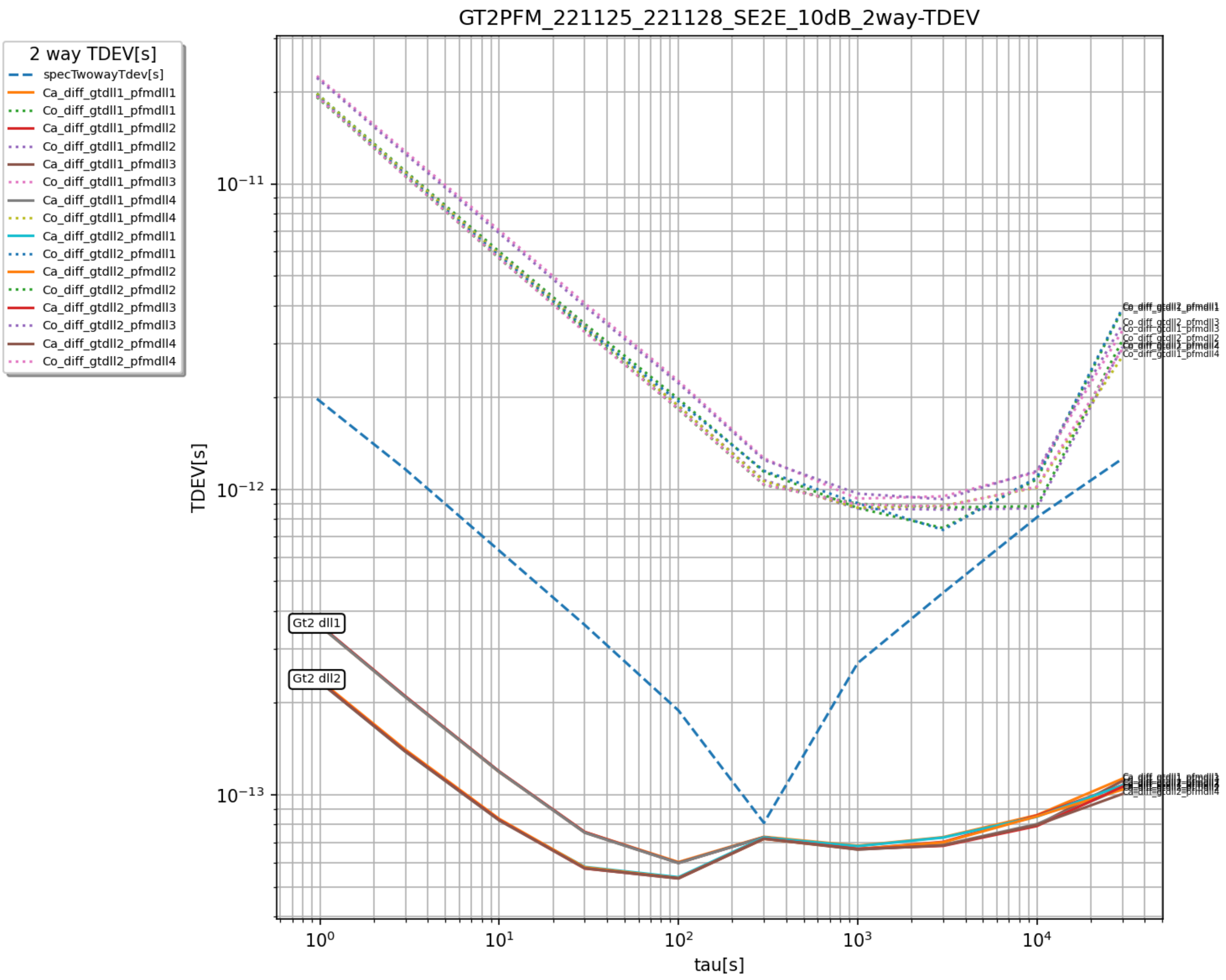

MWL PFM performance – Signal dynamics

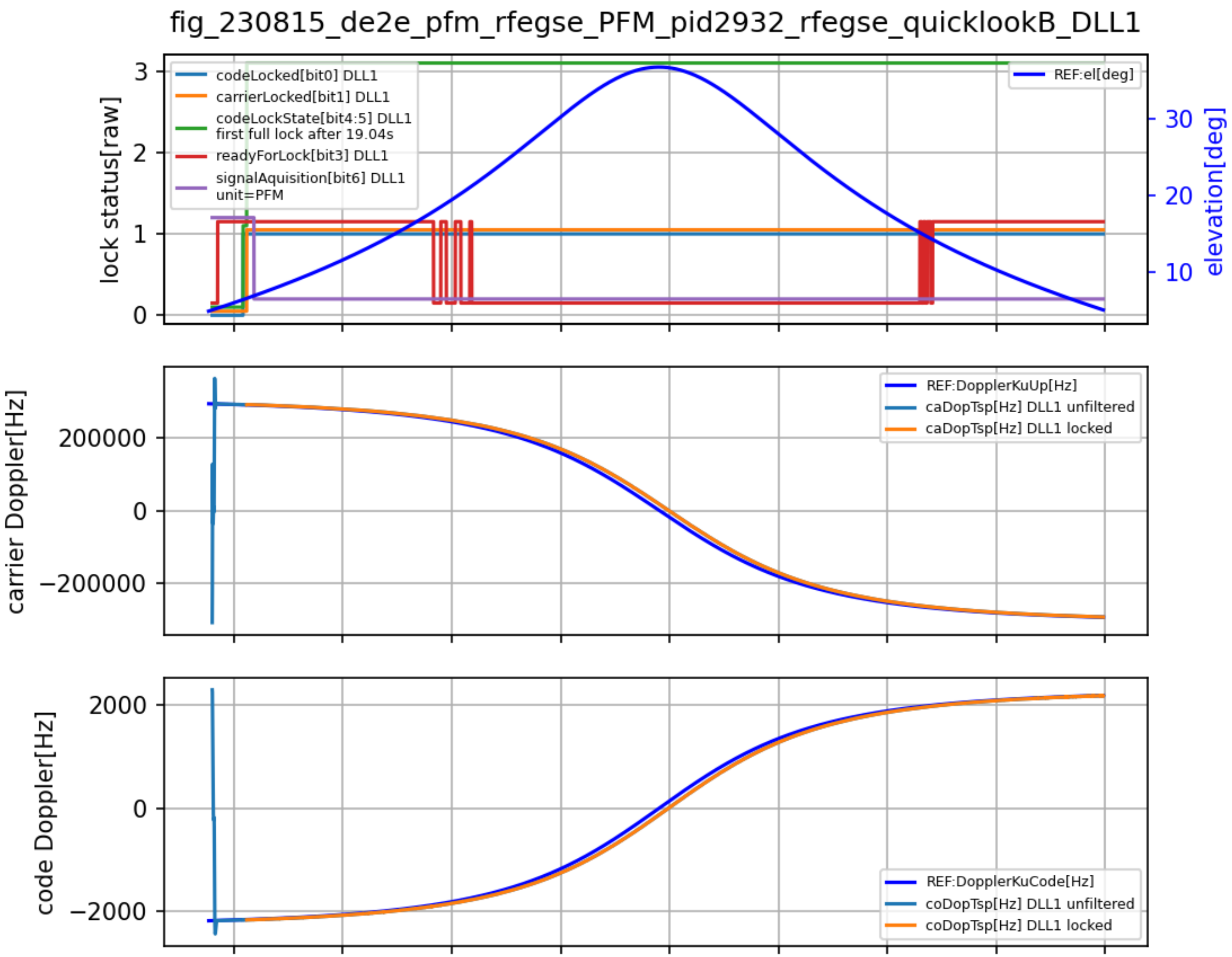

4 DLLs simultaneously tracking the same signal

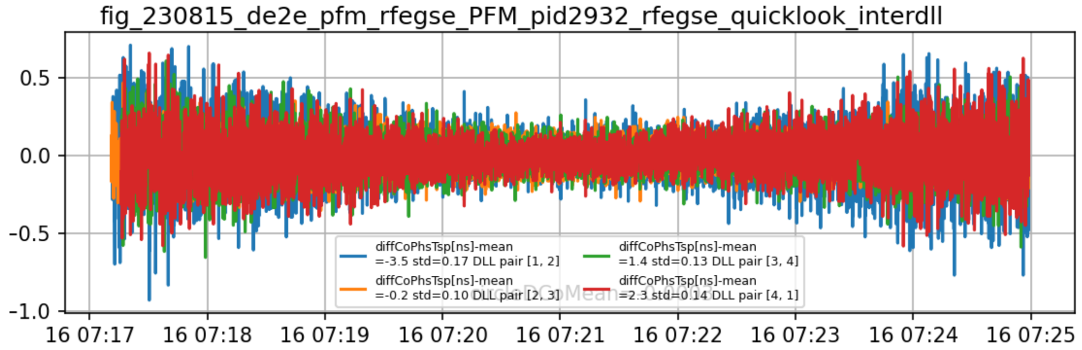

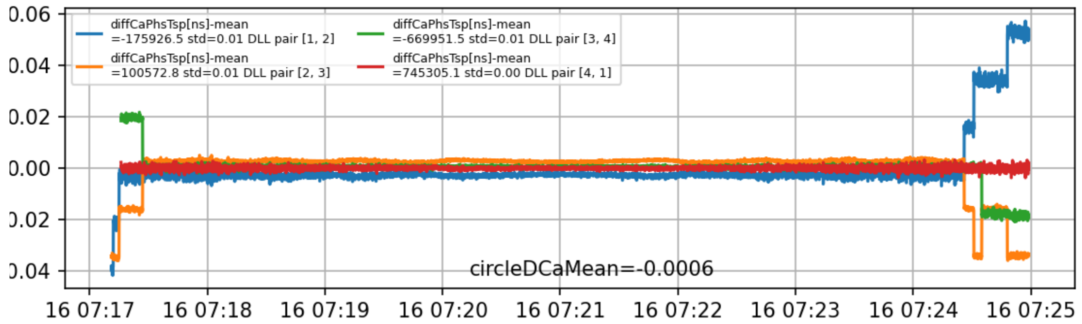

DLLx – DLLy code and carrier phase

MWL PFM performance – Signal dynamics

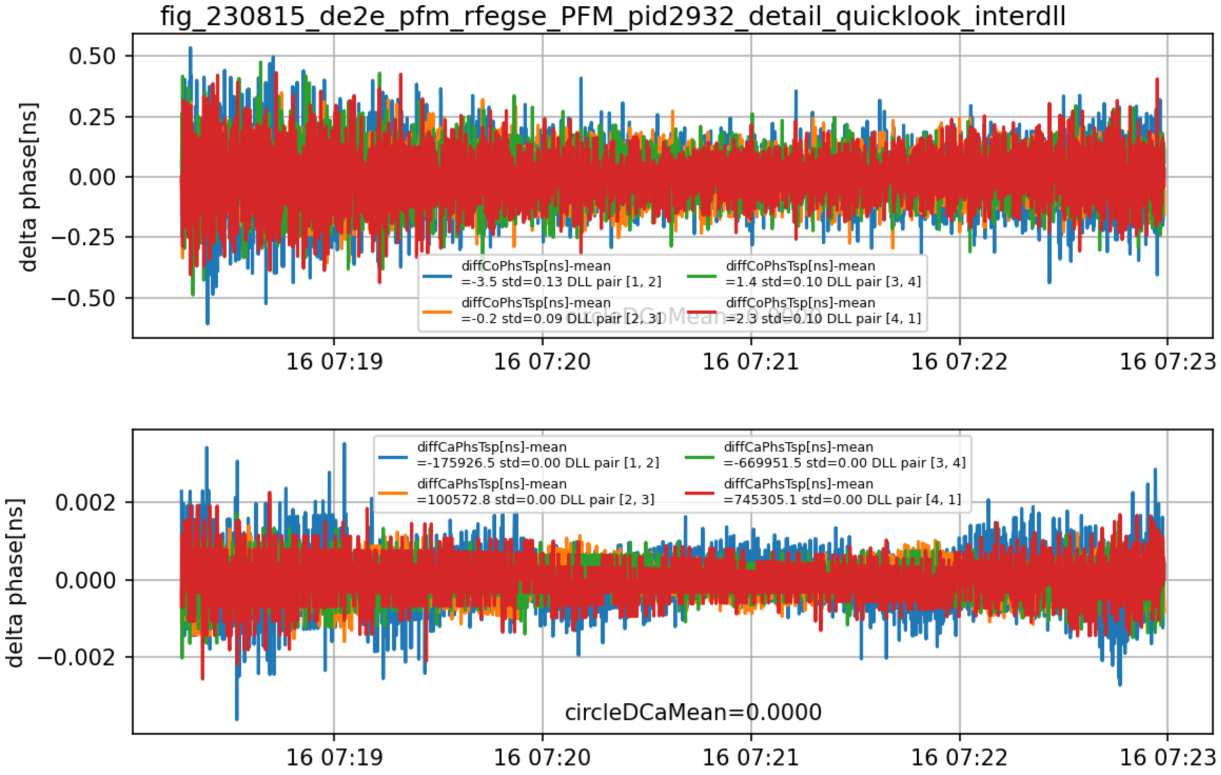

DLLx – DLLy code and carrier phase data after removing data containing carrier cycle slips

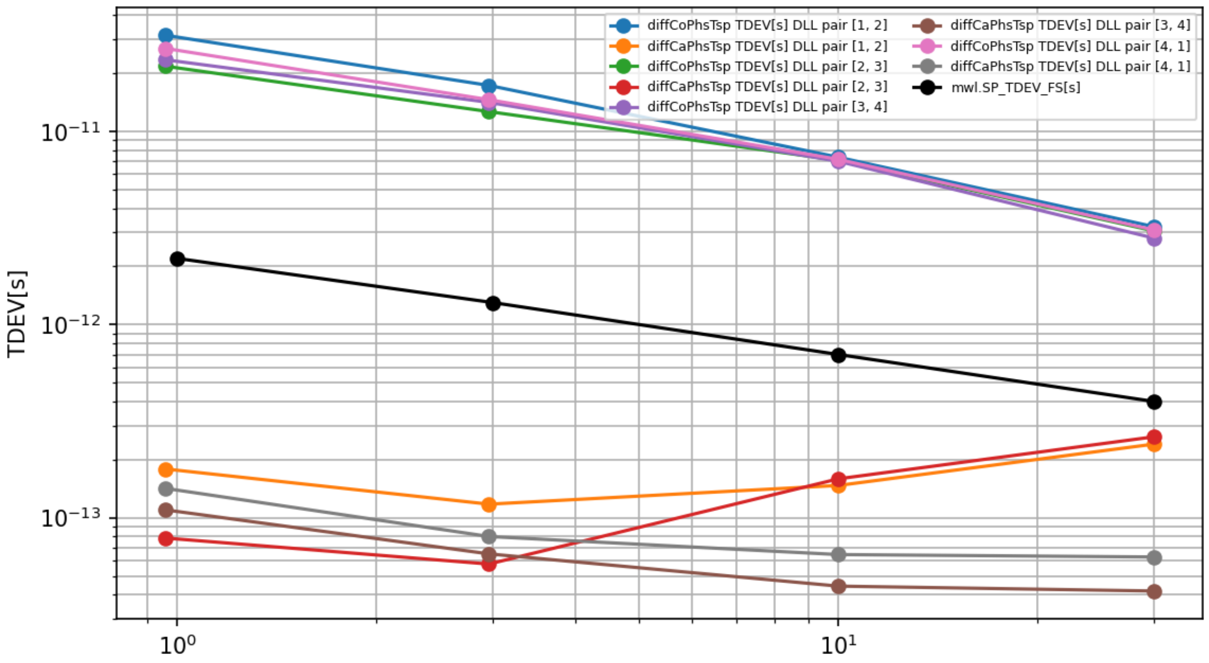

Time Deviation [s] of DLLx – DLLy code and carrier phase data

ACES MWL network

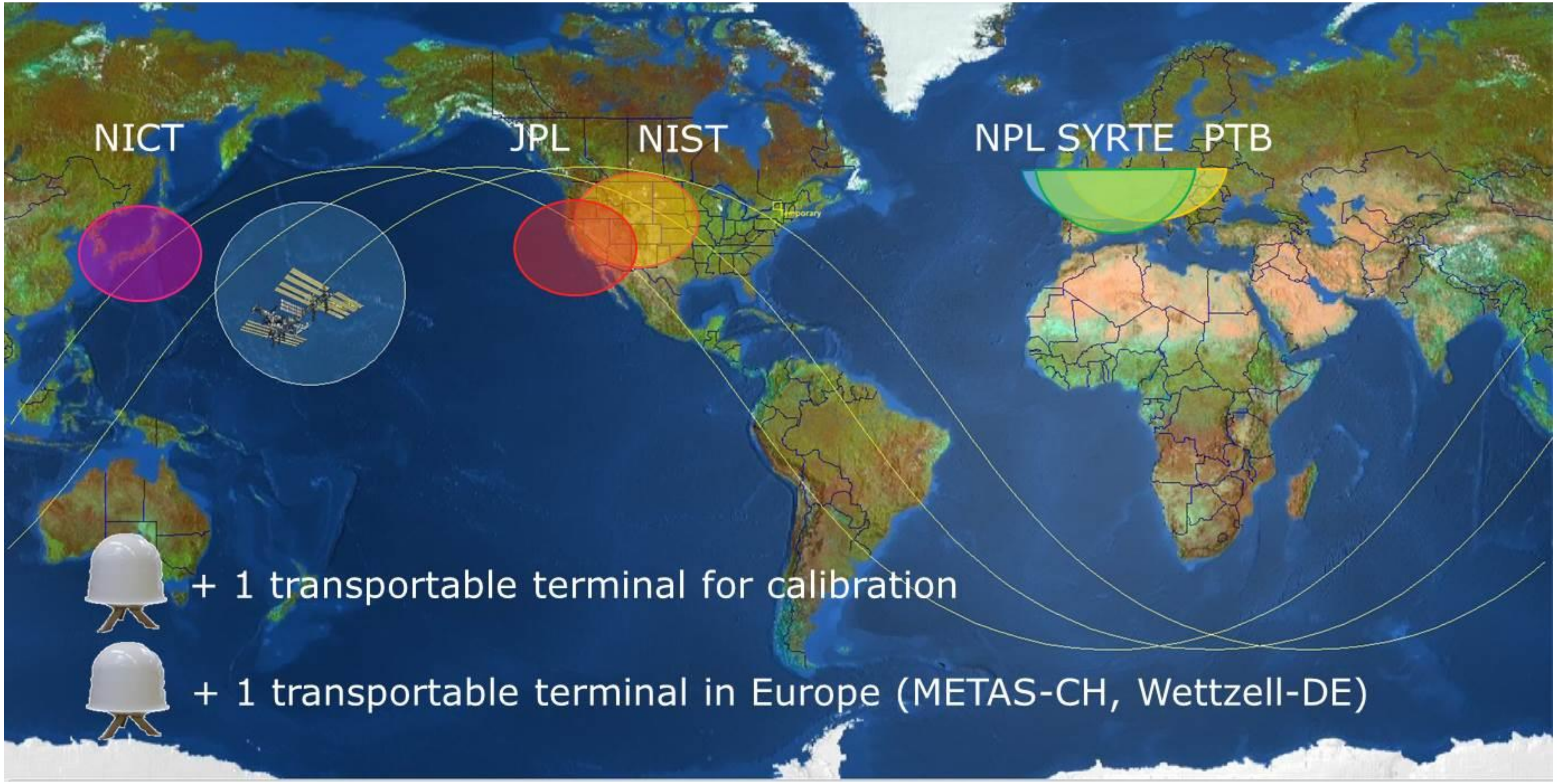

European Laser Timing (ELT)

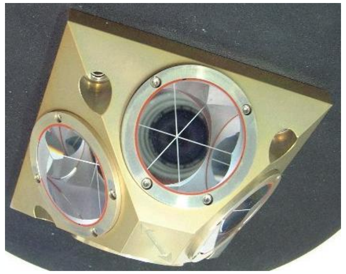

t_{space}

TM/TC

Power

ACES

ACES Time Scale (MWL)

t_{stop} t_{start}

$$\tau_g(t) - \tau_s(t) = \frac{t_{start} + t_{stop}}{2} - t_{space}$$
$$+\tau_{relativity} + \tau_{atmosphere} + \tau_{geometry}$$

CTU Prague

CSRC

TIMETECH

AIRBUS DEFENCE & SPACE

Detector package
500 grams
0.6 Watt

ELT performance - Preliminary

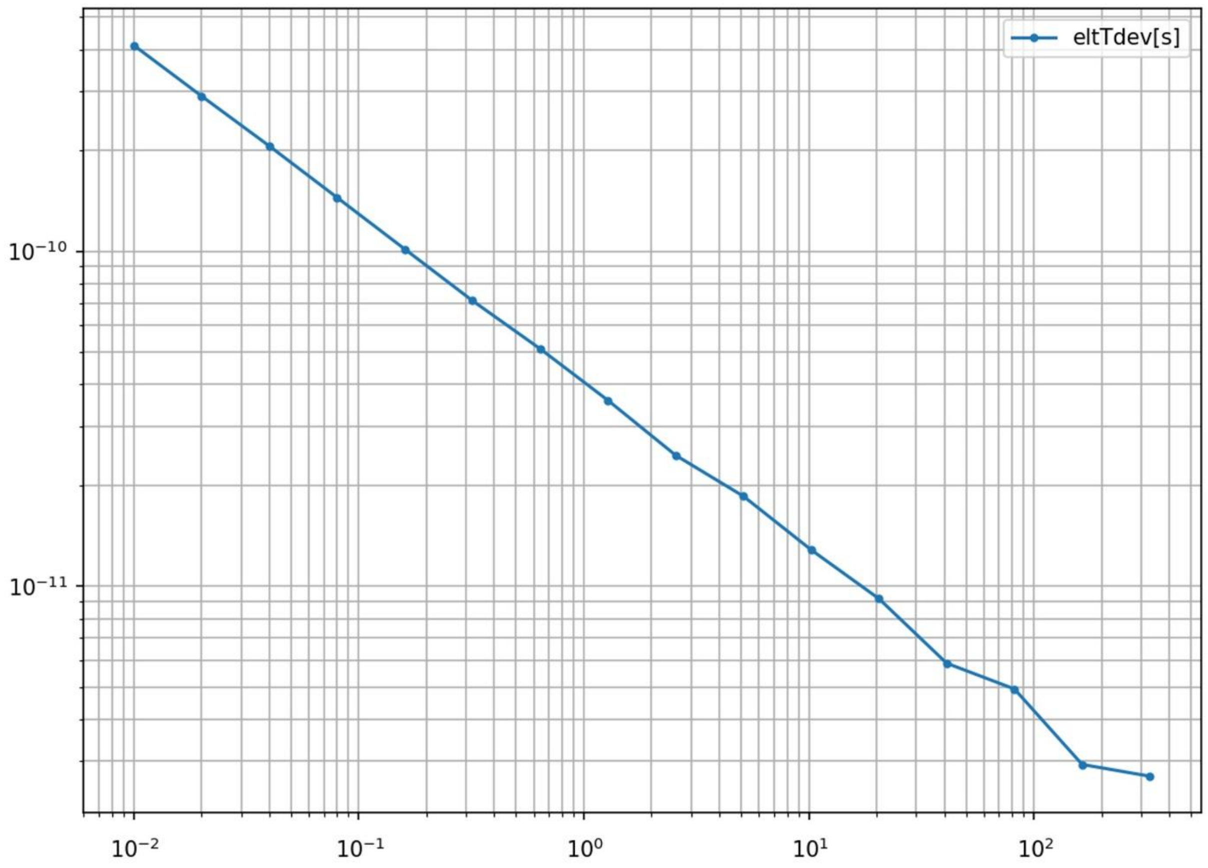

ELT Time Stability [s]: dark counts detection events vs NPET time tagging measurements at 100 Hz gate rate

ELT detector package tested from -55°C to +60°C: **K_T=1 ps/K**

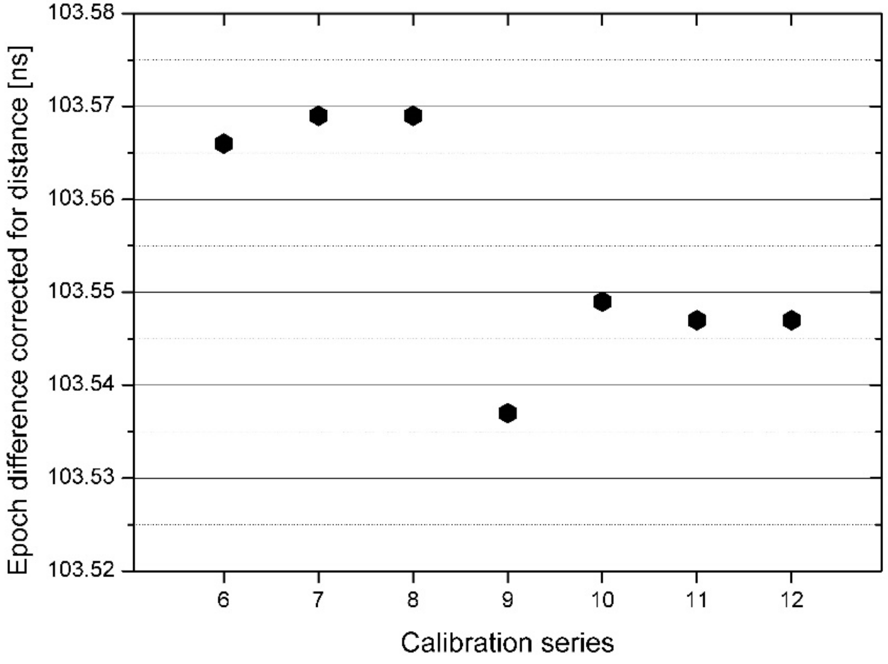

ELT Calibration Campaign at Graz SLR (1 yr)

ILRS network of SLR stations

esa

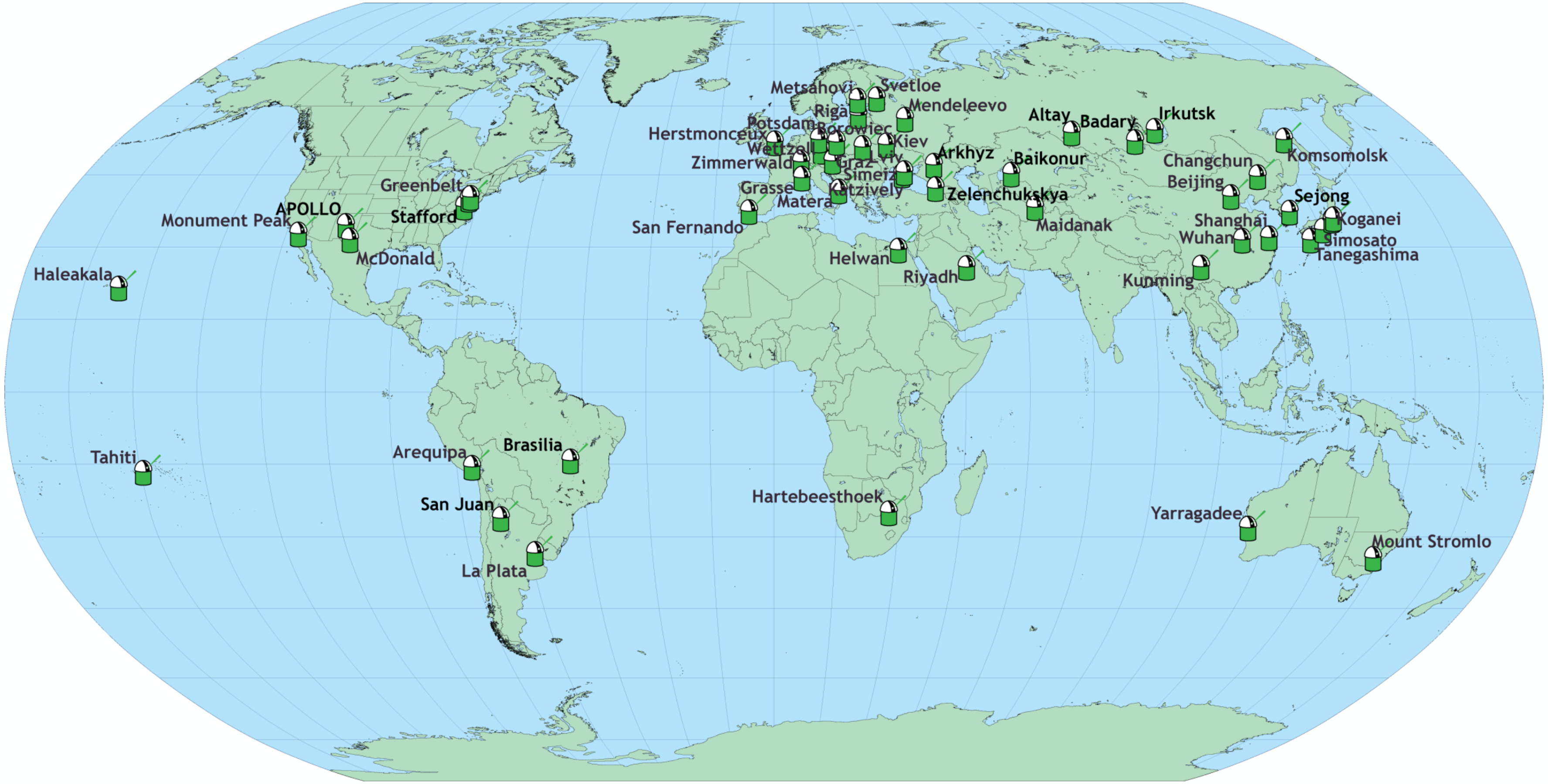

ACES as official ILRS target: Wettzell (primary station), Graz, Herstmonceaux, Potsdam, and Zimmerwald SLR stations already calibrated; other stations can join provided they comply with ISS safety requirements.

ACES – Fundamental Physics tests

ACES Mission Objectives	ACES performances	Scientific background and recent results
Gravitational red-shift	Absolute measurement of the gravitational red-shift to < $2 \cdot 10^{-6}$ after 10 days of integration time.	Factor 70 improvement over the GPA experiment and factor 10 over tests involving Galileo 5 and 6 satellites.
Time drifts of fundamental constants	Time variations of α constrained to $\alpha^{-1} \cdot d\alpha / dt$ < $3 \cdot 10^{-18}\ yr^{-1}$ after 3 years of mission.	Comparisons of clocks based on different atoms and atomic transitions on a worldwide scale to constrain α, m_e/Λ_{QCD} and m_q/Λ_{QCD}.
Dark matter search with atomic clocks	Establish bounds on topological dark matter models based on the comparisons of clocks in the ACES network.	Comparisons via the ACES network imposing limits on the three coupling constants Λ_α, Λ_e, and Λ_q in the model lLagrangian. Measurements over an interval T between encounters of 20 d. Simultaneous observation with several clocks along different baselines providing ways to confirm any observation above the sensitivity threshold and control the measurement systematics. Screening effect on the dark matter field due to the Earth mass reduced to about 0.06 on the space clock PHARAO with respect to ground clocks (~ 10^{-7}).

Gravitational redshift test

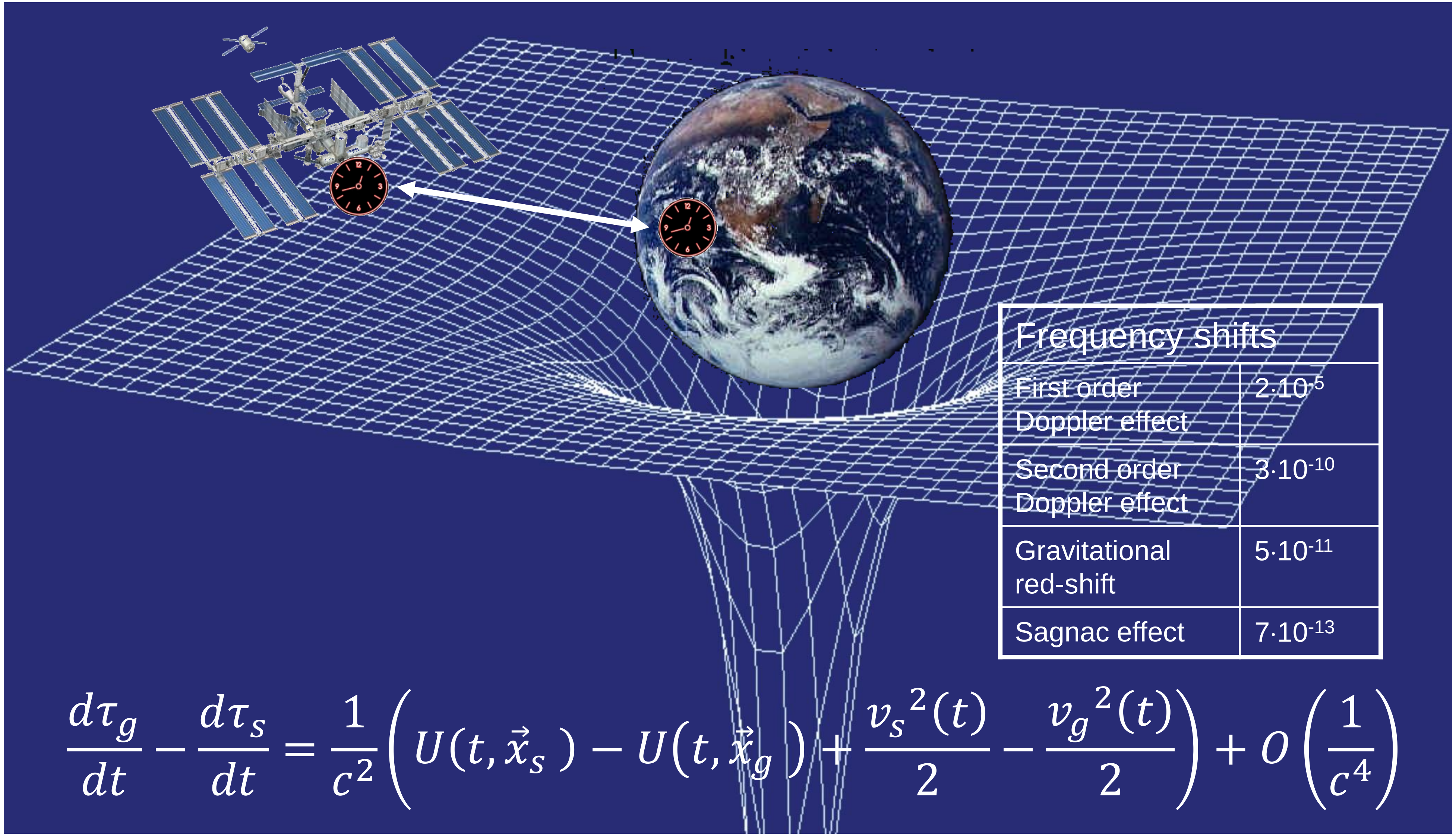

Frequency shifts	
First order Doppler effect	$2 \cdot 10^{-5}$
Second order Doppler effect	$3 \cdot 10^{-10}$
Gravitational red-shift	$5 \cdot 10^{-11}$
Sagnac effect	$7 \cdot 10^{-13}$

$$\frac{d\tau_g}{dt} - \frac{d\tau_s}{dt} = \frac{1}{c^2}\left(U(t,\vec{x}_s) - U(t,\vec{x}_g) + \frac{v_s{}^2(t)}{2} - \frac{v_g{}^2(t)}{2}\right) + O\left(\frac{1}{c^4}\right)$$

A network of atomic clocks to test fundamental physics

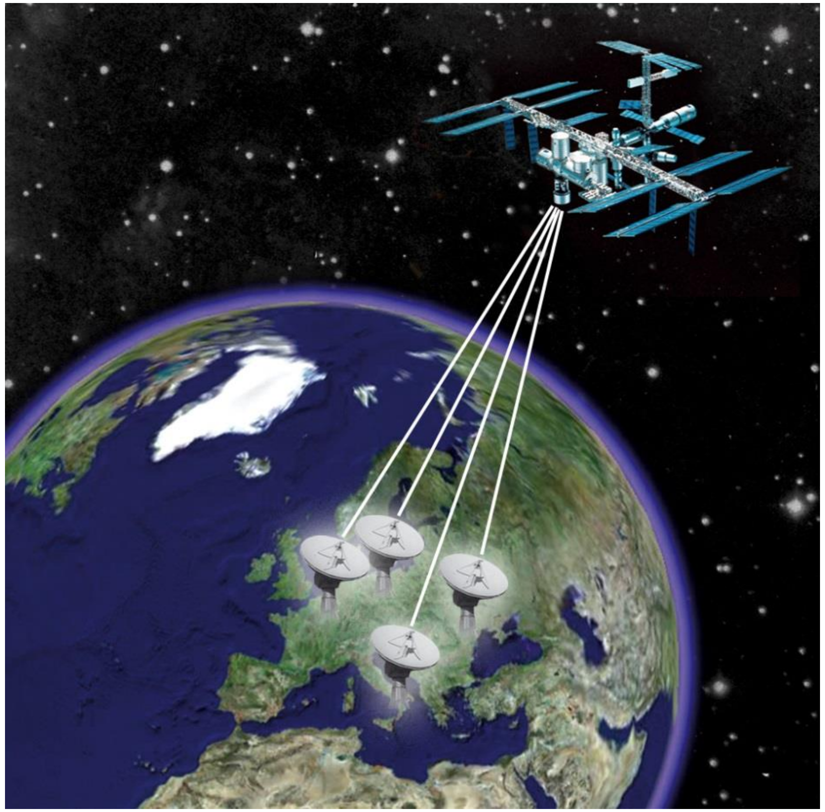

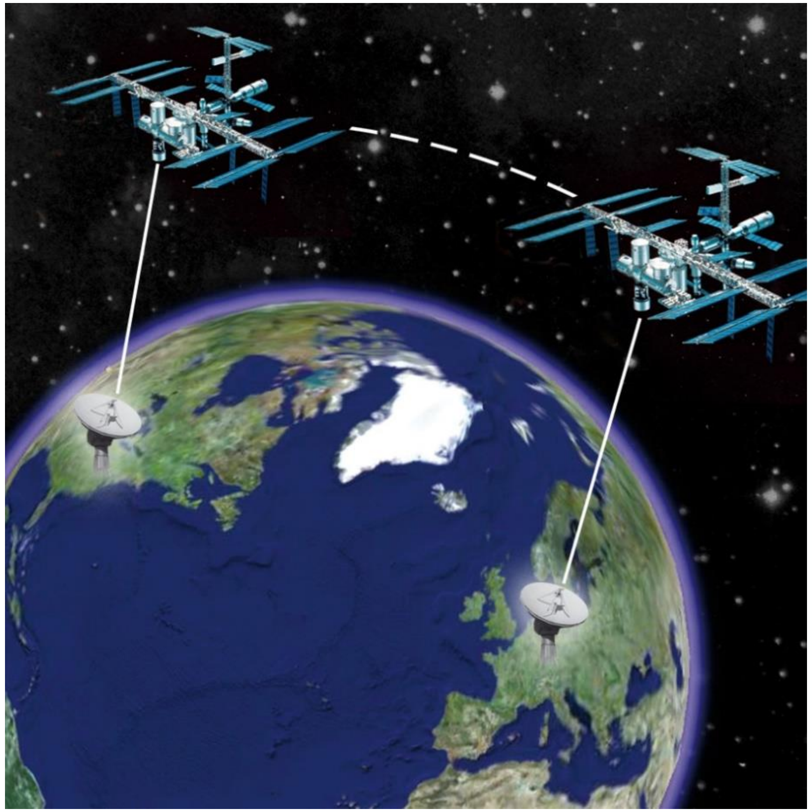

- ACES as a relay satellite to transfer time and frequency on a worldwide scale.
- Comparisons of ground clocks (microwave and optical) to better than $1 \cdot 10^{-17}$.

Time variations of fundamental constants

Frequency of hyperfine transitions: $\nu_{\rm hfs}^{(i)} \simeq R_\infty c \times \mathcal{A}_{\rm hfs}^{(i)} \times g^{(i)} \left(\frac{m_e}{m_p}\right) \alpha^2 F_{\rm hfs}^{(i)}(\alpha)$

Frequency of electronic transitions: $\nu_{\rm elec}^{(i)} \simeq R_\infty c \times \mathcal{A}_{\rm elec}^{(i)} \times F_{\rm elec}^{(i)}(\alpha)$

Ratios between atomic frequencies:

$$\frac{\nu_{\rm elec}^{(ii)}}{\nu_{\rm elec}^{(i)}} \propto \frac{F_{\rm elec}^{(ii)}(\alpha)}{F_{\rm elec}^{(i)}(\alpha)} \qquad \frac{\nu_{\rm hfs}^{(ii)}}{\nu_{\rm elec}^{(i)}} \propto g^{(ii)} \frac{m_e}{m_p} \alpha^2 \frac{F_{\rm hfs}^{(ii)}(\alpha)}{F_{\rm elec}^{(i)}(\alpha)} \qquad \frac{\nu_{\rm hfs}^{(ii)}}{\nu_{\rm hfs}^{(i)}} \propto \frac{g^{(ii)}}{g^{(i)}} \frac{F_{\rm hfs}^{(ii)}(\alpha)}{F_{\rm hfs}^{(i)}(\alpha)}$$

$g^{(i)}$ and m_p depend on the QCD mass scale Λ_{QCD} and $m_q = (m_u + m_d)/2$ thus

$$\delta \ln\left(\frac{\nu^{(i)}}{R_\infty c}\right) \simeq K_\alpha^{(i)} \times \frac{\delta\alpha}{\alpha} + K_q^{(i)} \times \frac{\delta(m_q/\Lambda_{\rm QCD})}{(m_q/\Lambda_{\rm QCD})} + K_e^{(i)} \times \frac{\delta(m_e/\Lambda_{\rm QCD})}{(m_e/\Lambda_{\rm QCD})}$$

$K_\alpha^{(i)} \neq 0, K_q^{(i)} \neq 0, K_e^{(i)} \simeq 1$ hyperfine transitions

$K_\alpha^{(i)} \neq 0, K_q^{(i)} \simeq 0, K_e^{(i)} \simeq 0$ electronic transitions

$K_\alpha^{(i)} \simeq 0, K_q^{(i)} \simeq 0, K_e^{(i)} \simeq 1/2$ vibrational transitions

V.V. Flambaum, Laser Spectroscopy, pp. 49-57 (2004)
V.V. Flambaum *et al.*, Phys. Rev. D **69**, 115006 (2004)

Dark matter search

- Atomic clock networks can be used to search for dark matter and place boundaries on certain models, e.g. topological dark matter (TDM).
- TDM is represented by a scalar field that couples to fundamental constants thus inducing fluctuations of atomic transition frequencies.
- The ACES network can ensure comparisons of atomic clocks based on different atomic transitions down to $1 \cdot 10^{-17}$, in the optical domain, in the microwave domain, and optical vs microwave.
- Limits on variations for each of the three fundamental constants can be established thus testing different terms in the model Lagrangian and imposing limits on the three energy scales Λ_α, Λ_e, and Λ_q.
- The simultaneous observation with several clocks compared along different baselines will provide ways to confirm any observation above the sensitivity threshold and control the measurement systematics.
- Clock comparisons can be performed continuously on 20 d intervals thanks to the ACES MWL, extending the time T between encounters.
- Screening effect of the dark matter field due to the Earth mass reduced to about 0.06 on the space clock PHARAO with respect to ground clocks (~ 10^{-7}).

ACES – Scientific applications

Relativistic geodesy

- Relativistic geodesy: mapping of the Earth gravitational potential based on the red-shift measured between two clocks at two different locations.
- ACES intercontinental comparisons of optical clocks at the 10^{-17} level after 4 days, corresponding to a resolution on the local height above the geoid at the 10 cm level.
- The global coverage offered by ACES will complement the results of the CHAMP, GRACE, and GOCE missions.

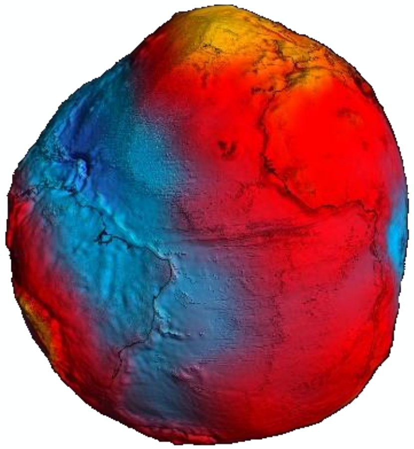

Clocks synchronization

- MWL and ELT clocks synchronization at the 100 ps and 50 ps level, respectively.

Atomic time scales (TAI)

- The PHARAO clock is accurate to $1\text{-}2{\cdot}10^{-16}$.
- MWL will provide means to compare atomic clocks on a worldwide scale:
  - PHARAO and primary standards on ground contributing to TAI.
  - Optical clock comparisons to $1{\cdot}10^{-17}$ will help SI second redefinition.

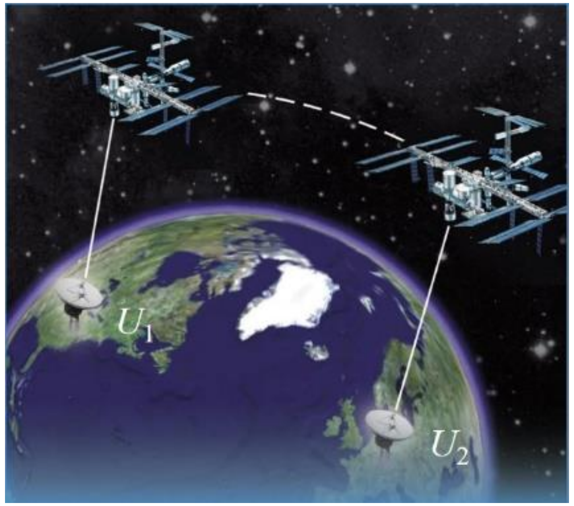

Way-forward to the ACES launch

- A first run of the ACES Integrated System Tests (IST) tests has been completed. They included:
  - ACES servo-loops performance
  - ACES clock signal performance evaluation
  - Sensitivity under temperature and magnetic field variations
- IST revealed a major anomaly: SHM getters had reached end-of-life and needed replacement.
- Acceptance status of ACES:
  - PHARAO clock PFM, ELT detector package, ACES GNSS system and FCDP PFM are integrated.
  - SHM PFM getters have been replaced and acceptance tests completed. SHM is now integrated in the ACES payload.
  - MWL PFM is completing qualification tests before final acceptance (by end 2023).
  - ACES payload performance tests planned for summer 2024.
- ACES PFM delivered for launch on SpaceX in end 2024 – beginning 2025.
- MWL GTs deployment will start in mid 2024 (SYRTE, PTB and Wettzell); the other institutes will follow.

L. Cacciapuoti[1], M. Armano[1], R. Jansen[1], R. Much[1], S. Weinberg[1], P. Crescence[2], A. Helm[2], J. Kehrer[2], S. Koller[2], R. Lachaud[2], T. Niedermaier[2], F.X. Esnault[3], D. Massonnet[3], J. Pittet[4], P. Rochat[4], S. Liu[5], W. Schaefer[5], T. Schwall[5], I. Prochazka[6], A. Schlicht[7], U. Schreiber[7], P. Delva[8], P. Laurent[8], M. Lilley[8], P. Wolf[8], C. Salomon[9]

[1]*European Space Agency, ESTEC, Noordwijk, The Netherlands*
[2]*Airbus Defence and Space, Friedrichshafen, Germany*
[3]*CNES, Toulouse, France*
[4]*Orolia Switzerland (Spectratime), Neuchâtel, Switzerland*
[5]*Timetech, Stuttgart, Germany*
[6]*Czech Technical University in Prague, Prague, Czech Republic*
[7]*Technical University of Munich, Munich, Germany*
[8]*SYRTE, Observatoire de Paris-PSL, CNRS, Sorbonne Université, LNE, Paris, France*
[9]*Laboratoire Kastler Brossel, ENS, Paris, France*

European Space Agency

Technical University of Munich

CTU CZECH TECHNICAL UNIVERSITY IN PRAGUE